Colloids and Surfaces B: Biointerfaces 169 (2018) 356–365

Contents lists available at ScienceDirect

Colloids and Surfaces B: Biointerfaces

journal homepage: www.elsevier.com/locate/colsurfb

Engineering PCL/lignin nanofibers as an antioxidant scaffold for the growth of neuron and Schwann cell

Jing Wang[a,b], Lingling Tian[b], Baiwen Luo[c], Seeram Ramakrishna[b], Dan Kai[d,*], Xian Jun Loh[d,e,f], In Hong Yang[c], G. Roshan Deen[g], Xiumei Mo[a,*]

[a] State Key Laboratory of Modification of Chemical Fibers and Polymer Materials, College of Chemistry, Chemical Engineering and Biotechnology, Donghua University, Shanghai 201620, China
[b] Center for Nanofibers and Nanotechnology, E3-05-14, Department of Mechanical Engineering, Faculty of Engineering, National University of Singapore, 2 Engineering Drive 3, 117576, Singapore
[c] Singapore Institute for Neurotechnology, National University of Singapore, 28 Medical Drive, #05-COR, 119077, Singapore
[d] Institute of Materials Research and Engineering (IMRE), A*STAR, 2 Fusionopolis Way. Innovis, #08-03, 138634, Singapore
[e] Department of Materials Science and Engineering, National University of Singapore, 9 Engineering Drive 1, 117576, Singapore
[f] Singapore Eye Research Institute, 11 Third Hospital Avenue, 168751, Singapore
[g] Soft Materials Laboratory, Natural Sciences and Science Education, National Institute of Education Nanyang Technological University, Singapore

ARTICLE INFO

Keywords:
Lignin
Ring-opening polymerization
Electrospinning
Neuron
Schwann cell

ABSTRACT

Antioxidant is critical for the successful of nerve tissue regeneration, and biomaterials with antioxidant activity might be favorable for peripheral nerve repair. Lignin, a biopolymer from wood with excellent antioxidant properties, is still "unexplored" as biomaterials. To design an antioxidative bioscaffold for nerve regeneration, here we synthesized lignin-polycaprolactone (PCL) copolymers via solvent free ring-opening polymerization (ROP). Then such lignin-PCL copolymers were incorporated with PCL and engineered into nanofibrous scaffolds for supporting the growth of neuron and Schwann cell. Our results showed that the addition of lignin-PCL enhanced the mechanical properties of PCL nanofibers and endowed them with good antioxidant properties (up to 98.3 ± 1.9% free radical inhibition within 4 h). Cell proliferation assay showed that PCL/lignin-PCL nanofibers increased cell viability compared to PCL fibers, especially after an oxidative challenge. Moreover, Schwann cells and dorsal root ganglion (DRG) neurons cultured on the nanofibers to assess their potential for nerve regeneration. These results suggested that nanofibers with lignin copolymers promoted cell proliferation of both BMSCs and Schwann cells, enhanced myelin basic protein expressions of Schwann cells and stimulated neurite outgrowth of DRG neurons. In all, these sustainable, intrinsically antioxidant nanofibers may be a potential candidate for nerve TE applications.

1. Introduction

Nervous system loses its functions due to disease, trauma, or aging [1,2]. Nerve damage is always in company with inflammation and oxidant stress [3]. Human nervous system is especially vulnerable to oxidant stress-related injury due to many reasons, including high oxygen consumption, excessive reactive oxygen species (ROS) generation, rich in polyunsaturated fatty acids, special neuronal conduction and synaptic transmission activity (high Ca^{2+} traffic) [4]. Tissue engineered (TE) nerve grafts showed their potential as an alternative to autologous nerve grafts for peripheral nerve repair [5–7]. However, many synthetic polymeric biomaterials, such as polycaprolactone (PCL) and poly (lactic acid), always induces an inflammatory response, triggers oxidant stress and generates ROS and other radicals in local tissue. The overdose of ROS can cause the damage of cell membrane lipids, proteins, and DNA, leading to the death of the grafted cells and failure of the implants. Therefore, nerve TE grafts with antioxidant properties maybe a suitable solution to overcome such issues. Different antioxidants including melatonin [8,9], acetyl-L-carnitine [10,11], β-carotene, Vitamin E and B-complex vitamins [12], were successfully applied for supporting the nerve repair by countervailing harmful effects of ROS. However, there are some limitations of all these traditional antioxidant agents, such as risk of enzymolysis, difficulty to reach the desired destination, and short half-life [13]. Biodegradable polymers with native intrinsic antioxidant potential may therefore provide another avenue for antioxidant therapy [14]. The nerve TE grafts

* Corresponding authors.
E-mail addresses: kaid@imre.a-star.edu.sg (D. Kai), xmm@dhu.edu.cn (X. Mo).

https://doi.org/10.1016/j.colsurfb.2018.05.021
Received 9 March 2018; Received in revised form 28 April 2018; Accepted 9 May 2018
Available online 12 May 2018

Table 1
Material characterization of PCL/lignin-PCL nanofibers.

Fibers	Copolymer blended	Feed ratio (PCL: LP)	Fiber diameter (nm)	Tensile strength (MPa)	Y modulus (MPa)	Elongation at break (%)
PCL	N.A.	100:0	383 ± 89	13.3 ± 1.1	24.0 ± 2.8	137 ± 16
PCL5LP2	LP2	95:5	338 ± 47	6.3 ± 1.1*	13.2 ± 1.4*	94 ± 22*
PCL10LP2	LP2	90:10	321 ± 56	10.0 ± 2.1*	16.7 ± 2.0*	160 ± 25
PCL15LP2	LP2	85:15	330 ± 49	8.4 ± 0.9*	16.1 ± 2.5*	116 ± 6*
PCL5LP4	LP4	95:5	214 ± 34*	9.8 ± 2.0*	24.7 ± 3.7	86 ± 16*
PCL10LP4	LP4	90:10	259 ± 42*	17.3 ± 1.8*	24.4 ± 2.9	160 ± 8*
PCL15LP4	LP4	85:15	289 ± 88	11.2 ± 2.5	22.8 ± 1.2	119 ± 15

* Significantly different from corresponding parameters of PCL fibers ($p < 0.05$).

contained this kind of polymers may have continuous local antioxidant property, as long as the polymer doesn't degrade completely.

Lignin is a well-known scavenger of oxygen free radical for stabilizing the reactions initiated by oxygen radicals [15]. This complex aromatic macromolecule contains large numbers of hydroxyl and methoxyl functional groups, which can donate hydrogen to terminate oxidation propagation reaction [16,17]. Many research groups have reported that lignin could be potentially used as antioxidant agents for healthcare applications [17–20], but still lignin is “rather unexplored” as biomaterials. In our previous studies, we designed and developed functional lignin-based materials and these materials exhibited excellent antioxidant properties and biocompatibility [21–24]. Here our aim is to evaluate the potential of lignin-PCL copolymer as a material for nerve tissue repair and regeneration.

In this study, we synthesized lignin-PCL copolymers (with different lignin content) via the solvent free ring-opening polymerization (ROP) of ε-caprolactone onto alkali lignin. Moreover, such anti-oxidative lignin-PCL copolymers were blended with PCL and then engineered into composite fibers via electrospinning. Electrospun nanofibers with similar structure of native extracellular matrix (ECM) have been regarded as a potential biomaterial graft for nerve TE [25–28]. PCL is a U.S. Food and Drug Administration (FDA) approved biodegradable polyester, while PCL based scaffolds have been widely used as scaffolds for various tissue engineering applications due to their biocompatibility, slow degradation rate, and ease of processing [29–34]. Thus, PCL was used as the matrix material and polymerized with lignin to obtain a copolymer which can overcome the shortcomings of the use of PCL and lignin alone including the mechanical property, biocompatibility and anti-oxidative damage ability. The topographical, mechanical properties and antioxidant activity of the blending nanofibers were evaluated. Furthermore, neurons and Schwann cells were cultured on the fibers to evaluate its growth behavior. Our hypothesis is that such lignin-PCL copolymers could provide mechanical reinforcement and antioxidant properties to the resulting nanofibers, which might increase the viability of nerve cells against oxidant stress, and promote neurite outgrowth of neurons and Schwann cells growth for nerve regeneration.

2. Materials and methods

2.1. Materials

All chemicals were purchased from Sigma-Aldrich Chemicals and used as received except where noted. The average Mn of Polycaprolactone (PCL) was 80,000. Alkali lignin (Mn = 5000 g/mol) was dried at 105 °C overnight before use. Rat Schwann cells (S42 ATCC® CRL2942™) were obtained from ATCC, USA, while Schwann cell culture medium was purchase from Gene-Ethics Asia Pte Ltd, Singapore. Human bone marrow mesenchymal stem cells (PT 2501) were obtained from Lonza, Switzerland. Fetal bovine serum (FBS), trypsin/EDTA and Neurobasal Medium and B27 supplement factors were all purchased from GIBCO Invitrogen, USA. Alamar Blue (AbDSerotec) was purchased from Chemoscience, Singapore, and nerve growth factor (NGF) was purchased from Millipore, Singapore. All chemicals were of analytical grade and used without further purification.

2.2. Synthesis of lignin-PCL copolymers

Lignin-PCL was synthesized by a solvent free polymerization. For example, alkila lignin (4 g), ε-caprolactone (6 g) and Tin(II) 2-ethylhexanoate (0.5 wt% of monomer as catalyst) were added into a round bottomed flask. After purging with N_2 for 30 min, the mixture was stirred at 130 °C for 24 h. Then the mixture was cooled down to room temperature and dissolved with 100 ml of chloroform. The synthesized lignin-PCL copolymers will be dissolved in chloroform, and unreacted lignin will be removed by centrifugation (5000 rpm for 5 min). The supernatant was poured into excess hexane, and the precipitate (lignin-PCL) was collected and dried in vacuum oven at 50 °C for 24 h. 2 different PCL−lignin copolymers were synthesized under similar conditions by varying the feeding ratio of lignin: ε-caprolactone (2: 8 and 4: 6) as shown in Table 1.

2.3. Characterization of lignin-PCL copolymers

Lignin-PCL copolymer was analyzed by ^{1}H NMR (Bruker 400 MHz). Deuterated chloroform ($CDCl_3$) was used as a solvent to dissolve synthesized materials. Molecular weight and polydispersity index of polymer sample were analyzed by Waters gel permeation chromatography (GPC, a Shimadzu SCL-10A and LC-8A system equipped with two Phenogel 5 mm 50 and 1000 Å columns in series and a Shimadzu RID-10A refractive index detector) by using HPLC tetrahydrofuran as an eluent. The flow rate of tetrahydrofuran eluent was 1.0 ml/min at 25 °C. The number average molecular weights (M_n), weight average molecular weights (M_w) and polydispersity index (PDI, M_w/M_n) were determined with a calibration based on linear poly(methyl methacrylate) standards. Thermal behaviors of the copolymers were also investigated. Thermogravimetric analysis (TGA) was carried out on a thermogravimetric analyzer (Q500, TA Instruments, USA). Samples were heated at 20 °C/min from room temperature to 700 °C in a dynamic nitrogen atmosphere (flow rate = 60 ml/min). DSC thermal analysis was performed on a differential Scanning Calorimeter (DSC, Q100, TA Instruments, USA) equipped with an auto cool accessory and calibrated using indium. The following protocol was used for each sample: heating from −80 °C to +150 °C at 20 °C/min, holding at +150 °C from 5 min, cooling from +150 °C to −80 °C at 20 °C/min, and finally reheating from −80 to +150 °C at 20 °C/min. Melting temperatures and melting enthalpy change (ΔH_m) was determined from the endothermic melting peak.

2.4. Electrospinning of PCL/lignin-PCL nanofibers

PCL along with lignin-PCL copolymers were dissolved in 1, 1, 1, 3, 3, 3-hexafluoro-2-propanol (HFP). The mass ratios of PCL and each lignin-PCL copolymer were 95:5, 90:10 and 85:15. The total concentration of the solution was 10% (w/v). The electrospinning process was the same as described in the previous work [35]. The solution was pumped out at 1 ml/h with 15 kV of voltage applied on the needle. The

formed fibers were collected onto an aluminum foil covered platform. (10 cm away from the needle tip). The fabricated fiber mats were dried overnight in vacuum oven. Neat PCL fibers were fabricated under the same parameters as control. PCL nanofibers with 10% (w/w) Vitamin E (10% VE in PCL) labeled as PCL10VE were also fabricated as the control group. In detail, PCL was dissolved in HFP at a concentration of 10% w/v. Then VE, which accounted for 10% of the mass of PCL, was added to the solution. After stirring, the fibers were fabricated under the same parameters described above.

2.5. Characterization of electrospun fibers

The surface topographies of the fibers were characterized by scanning electron microscopy (SEM, JSM6700F, JEOL, Japan). The average diameter of fibers was calculated from 50 random fibers based on the image with Image J software (National Institutes of Health, Bethesda, USA).

Mechanical property of nerve TE grafts is an essential aspect which should be considered in nerve regeneration. A favorable nerve graft should mechanically match the strength of natural nerves to withstand physiological loads. The mechanical properties of the PCL/lignin-PCL fibers were measured by using uniaxial tensile testing technique (Instron 5943, USA) with 10 N load capacity with a rate of 10 mm/min. 5 pieces were prepared for each samples.

The antioxidant activity of lignin-PCL copolymers and PCL/lignin-PCL fibers was assessed by 1,1-diphenyl-2-picrylhydrazyl (DPPH) assay [36,37]. Lignin-PCL copolymers (10 mg) and fibers (20 mg) were placed in glass vials. Pure PCL and Vitamin E of the same weight as Lignin-PCL copolymers were used as control. A 60 μM DPPH solution in MeOH was prepared, and 10 ml of such solution was added into each vial. DPPH free radical content was measured by monitoring the absorbance changes at 517 nm at each time point. All samples were prepared in triplicate. The antiradical activity was measured as% inhibition of free radicals by measuring the decrease in absorbance compared to control solutions.

2.6. The evaluation of nanofiber biocompatibility

Bone marrow mesenchymal stem cell (BMSC) is one of the most commonly used seed cells in nerve tissue engineering [38,39]. Therefore, the viability of BMSCs on the nanofibers was used to evaluate the biocompatibility of different nanofibers. The circular nanofiber mat with a diameter of 15 mm was placed in 24-well plate and pressed with a stainless steel ring to ensure complete contact of the scaffolds with wells. And then the nanofiber mats were washed thrice with PBS after sterilization with UV light. Subsequently, all samples were immersed in culture medium before cell seeding. The cells were seeded on nanofiber mat at a density of 10^4 cells per well.

The proliferation viability of BMSCs was determined by Alamar blue assay after 5 and 10 days of culture. In detail, the medium was removed and 1 ml 10% Alamar blue solution (10% Alamar blue, 90% pure medium without FBS) were added to each well and then incubated for further 4 h at 37 °C. The mixture solution was pipetted into 96-well plate and obtained the fluorescence intensity using a Thermo Scientific Microplate Reader (Varioskan Flash Multimode Reader, Thermo Scientific).

2.7. The oxidative stress in cells on nanofibers

To investigate the protective effect of nanofibers on oxidative-stress damage in nerve cells, Schwann cells were seeded on sterilized PCL/lignin nanofibers at a density of 2×10^4 cells per well. And PCL nanofibers with 10% (w/w) Vitamin E (10% VE in PCL) labeled as PCL10VE was fabricated as the control group to evaluate the oxidation resistance of lignin containing fibers. Then the cells were treated with hydrogen peroxide (H_2O_2), a typical oxidative stress inducer, known to induce rapid cell death due to excessive ROS generation. In detail, the cells were treated with H_2O_2 (200 μM in PBS) for 20 min after seeding overnight. Then the H_2O_2 solution was removed and the cells were rinsed thrice with PBS. Fresh cell culture medium was added and cultured in incubator at 37 °C. The cell viability was performed with Alamar blue after 1 and 3 days of incubation.

2.8. Cell behavior of Schwann cells on electrospun nanofibers

Schwann cells play a critical role in neuron survival and nerve regeneration [40,41]. In order to evaluate the behavior of Schwann cells on different nanofibers, the proliferation was performed after 1, 3, 5 days of culture by Alamar blue assay as described above. Additionally, the morphology of Schwann cells on different nanofibers was also observed after 7 days of culture. The samples were treated with formalin solution for 20 min, washed thrice with PBS and dehydrated with a series of graded ethanol solutions (50%, 70%, 90% and 100%) for 15 min each. Then, all samples were treated with HDMS and air-dried overnight. Finally, the morphology of cells were visualized under SEM after sputter coating with gold.

2.9. Expression of myelin basic protein (MBP) on electrospun nanofibers

To evaluate the influence of different nanofibers on expression of myelination related proteins of Schwann cells, the MBP expression was determined with immunostaining. After 7 days of culture, all samples were rinsed with PBS, fixed with formalin for 20 min and treated with 0.1% Triton-X100 for permeabilization for 5 min. Then 3% BSA solution was used to block nonspecific binding for 90 min. Next, the cells were stained with anti-MBP antibody produced in rabbit at a dilution of 1:200 overnight at 4 °C. Subsequently, all samples were washed thrice with PBS and stained with FITC conjugated goat anti rabbit at a dilution of 1:300 for 1 h. After rinsing with PBS for five times, the samples were treated with mounting medium with DAPI (Vector Laboratories, USA). Finally, the immunostained samples were visualized under laser scanning confocal microscopy (LSCM) to observe the cell phenotype.

2.10. Neurite outgrowth of DRG neurons on electrospun nanofibers

DRG neurons were isolated from the embryo of the 14 day pregnant rat. The neurons were seeded on nanofibrous scaffold in 24-well cell culture plate with a density of 20,000 per well. All nanofibrous mats for neurons seeding were sterilize under UV light for 5 h, followed by thrice rinse with PBS and immersion in culture medium. The culture medium for DRG neurons was Neuralbasal medium with 1% Penicillin-Streptomycin Solution, 2% B27 supplement factors and 20 ng ml^{-1} NGF. After 7 days of culture, the DRG neurons were treated with 4% paraformaldehyde for 30 min at 4 °C and then washed thrice with PBS. Subsequently, the DRG neurons were immunostained with the primary antibody solution (anti–160 kD neurofilament medium antibody, Abcam) overnight at 4 °C. The samples were incubated with Goat anti-mouse IgG H&L (Alexa Fluor 488, Abcam) after washing with PBS for three times. The nuclei was stained with DAPI (Thermo Scientific) for 15 min. The immunostained DRG neurons were visualized under LSCM. The neurite length was measured using Image J software and the mean values were then calculated.

2.11. Statistical analysis

All data were presented as mean ± standard deviation, and Student's *t*-test and one-way ANOVA were used in statistical analysis. Differences between the groups are considered statistically significant at $p < 0.05$.

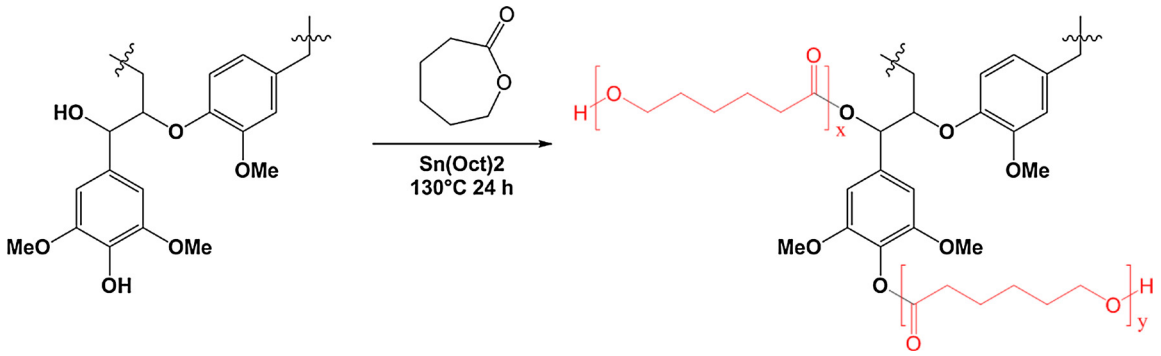

Fig. 1. Synthetic route for lignin-PCL copolymers via a solvent free polymerization.

3. Results and discussion

3.1. Synthesis and characterization of lignin-PCL copolymers

Lignin is brittle and incompatible with many other polymer systems, and therefore chemical modification of lignin is considered as an effective approach to engineering functional lignin-based composites. In this study, we synthesized lignin-PCL copolymers via the solvent free ROP of ε-caprolactone onto alkali lignin (Fig. 1). Fig. 2 shows the representative NMR spectrum of lignin-PCL copolymer. The characteristic chemical shifts of lignin were observed at 3.85 ppm corresponding to methoxyl protons and 6.85 ppm presenting the protons of the phenyl ring. The appearance of strong signals was detected at 2.30 ppm, 1.62 ppm, 1.35 ppm and 4.05 ppm corresponding to the α-, β-, γ-, and ε-methylene protons in PCL chains, respectively. Also the end group of PCL (peak g) was observed at 4.21 ppm. Based on the integration of peak d and f, the average PCL chain lengths in the copolymers could be calculated as n = 23.5 for LP2 and 3.4 for LP4, respectively (Table S1).

The molecular weight of lignin-PCL copolymer was analyzed by GPC. As shown in Table S1, LP2 (the mass feed ratio of lignin:CL was 2:8) showed the M_n of 12.0 kDa and M_w of 32.5 kDa, while LP4 (the mass feed ratio of lignin:CL was 4:6)chains displayed the M_n of 7.5 kDa and M_w of 10.5 kDa. Based on the molecular weight of lignin (Mn = 5 kDa), the mass% of lignin in copolymers were 41.7% for LP2 and 66.7% for LP4, respectively. DSC curves showed an interesting result (Fig. 3). LP2 with long PCL chains is a semi-crystalline polymer with a glass transition temperature (T_g) of −17 °C, a melting temperature (T_m) of 48 °C and ΔH_m of 61.9 J/g. On the other hand, LP4 displayed an amorphous properties with two different T_g (–15 °C and 108 °C) attributed by PCL segments and lignin segment, respectively. All above results confirmed that the PCL chains were successfully grafted onto the lignin core.

3.2. Electrospinning and characterization of PCL/lignin-PCL nanofibers

The lignin-PCL copolymers combined with PCL were engineered into composite fibers via electrospinning. The morphology and the diameter distribution of different nanofibers were shown in Fig. 4 and Table 1. The average diameters of PCL5LP2 (5% LP2 in PCL), PCL10LP2 (10% LP2 in PCL), and PCL15LP2 (15% LP2 in PCL) nanofibers were

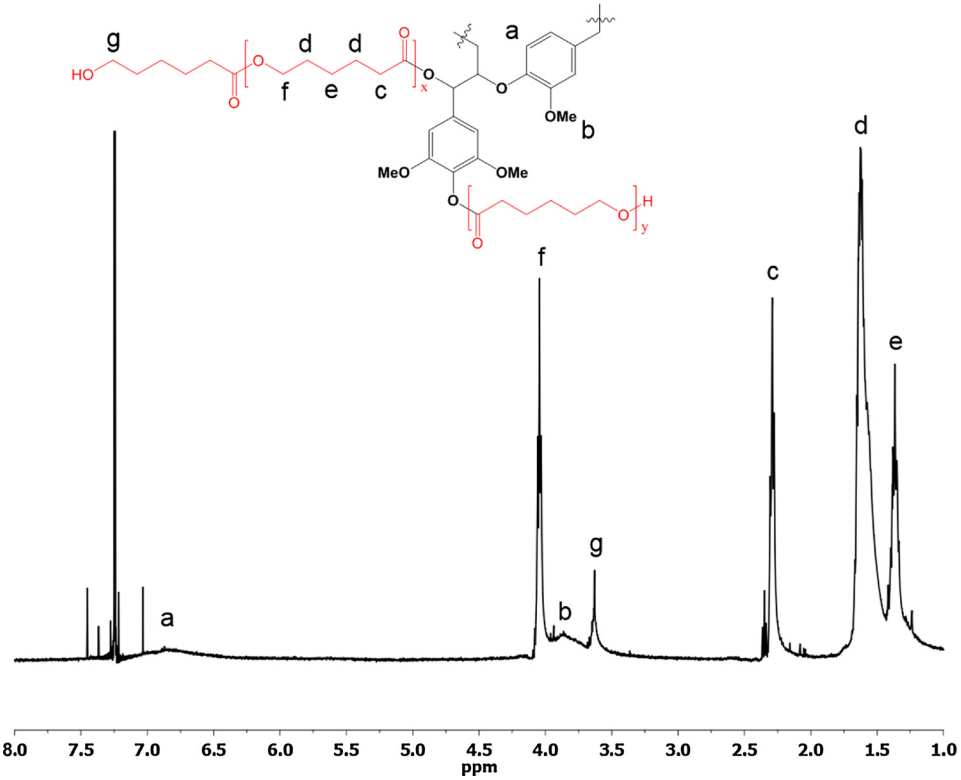

Fig. 2. ^{1}H NMR spectrum of lignin-PCL copolymer in $CDCl_3$.

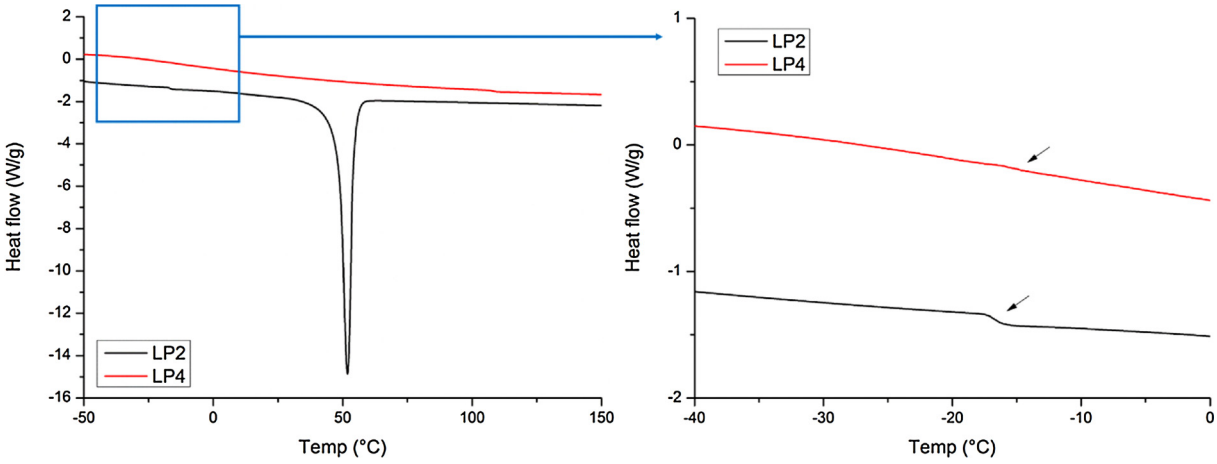

Fig. 3. DSC curves of lignin-PCL copolymers.

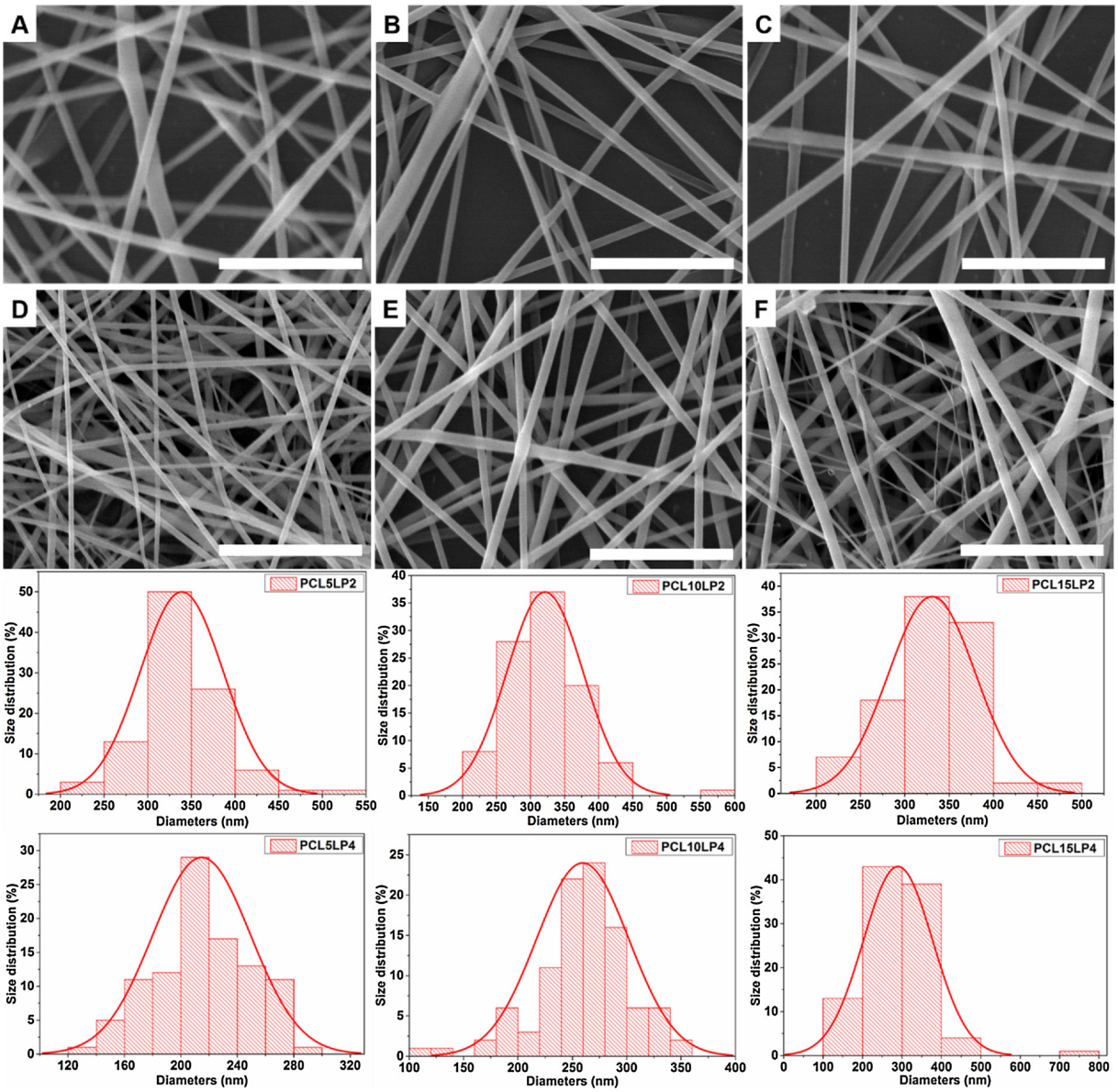

Fig. 4. SEM images and diameter distribution of different nanofibrous scaffold. A-C: PCL5LP2, PCL10LP2, PCL15LP2; D-E: PCL5LP4, PCL10LP4, PCL15LP4. The scale bar is 5 μm.

338 ± 47, 321 ± 56, and 330 ± 49 nm, respectively. There was no significant difference between three groups of values, indicating that there was no significant effect on fiber diameters with the increase of LP2 content from 5% to 15%. As for the nanofibers containing LP4, the average diameters of PCL5LP4 (5% LP4 in PCL), PCL10LP4 (10% LP4 in PCL), and PCL15LP4 (15% LP4 in PCL) were respectively 214 ± 34, 259 ± 42, 289 ± 88 nm, indicating that the fiber diameter increased with increasing of LP4 content. Compared with the average diameter (383 ± 89 nm) of pure PCL nanofibers, the average diameters of nanofibers reduced with the addition of copolymer LP2 and LP4.

The results of mechanical test were summarized in Table 1. Typical stress–strain curves of the PCL/lignin-PCL nanofibers were shown in Fig. S1. Neat PCL nanofibers displayed elastic mechanical properties (tensile strength of 13.3 ± 1.1 MPa; Young's modulus of 24.0 ± 2.8 MPa and elongation at break of 137 ± 16%).The addition of the copolymer LP2 significantly reduce the mechanical properties of the resulting nanofibers. PCL5LP2 showed the lowest tensile strength of 6.3 ± 1.1 MPa and Young's modulus of 13.2 ± 1.4 MPa among all the nanofibers. On the other hand, PCL10LP4 with 10% amorphous copolymer LP4 exhibited reinforced tensile strength (17.3 ± 1.8 MPa) and elongation at break (160 ± 8%) compared to pure PCL nanofibers. It is reported that the elastic modulus and ultimate tensile strength of intact human nerve were 15.87 ± 2.21 MPa and 6.78 ± 0.57 MPa, respectively [42]. Therefore, the mechanical properties of all scaffolds satisfied the requirement of nerve tissue engineering especially for those LP2 nanofibers.

The result of DPPH assay was shown in Fig. 5A. PCL showed very low antioxidant activities with 11.5 ± 3.4% free radical inhibition, while both copolymers exhibited good antioxidant properties. LP2 showed the free radical inhibition of 47.9 ± 5.9%, which is similar to the antioxidant activity of vitamin E (VE, 43.2 ± 5.8%). LP4 with high content of lignin exhibited the highest free radical inhibition of 95.7 ± 0.3%. Lignin with high content of phenolic moieties exhibits good antioxidant activity. Fig. 5B shows the antioxidant activities of PCL/lignin-PCL nanofibers. Neat PCL nanofiber showed the lowest antioxidant activities. The incorporation of lignin copolymers improved the antioxidant activities of the nanofibers, and higher amount of lignin copolymers resulted in a higher free radical inhibition. Among all nanofibers, PCL15LP4 showed the highest free radical inhibition, which reached 98.3 ± 1.9% only after 4 h of incubation.

3.3. The biocompatibility of PCL/lignin-PCL nanofibers

As shown in Fig. 5C, the proliferation of BMSCs gradually increased on all the nanofibrous scaffolds. The cells on PCL10LP2 and PCL15LP2 nanofibers showed faster proliferation than that on PCL5LP2 nanofibers, while PCL10LP4 nanofibers resulted in better cell proliferation than PCL5LP4 and PCL15LP4. Overall, PCL10LP4 nanofibers showed the favorable properties for BMSCs growth.

3.4. The protection of fibers on oxidative-stress damage in Schwann cells

Implantation of artificial nerve grafts is always companied with inflammatory responses and oxidative stresses. Nerve cells under such condition would generate excessive nicotinamide adenine dinucleotide phosphate (NADPH) oxidases and ROS, which then cause DNA damage and necrosis [28]. Hence, it might be helpful of using such lignin-based antioxidative nanofibers to locally lessen oxidative stress for better cell viability. In order to further determine whether the nanofibers could lessen oxidative stress for better nerve cell viability, Schwann cells

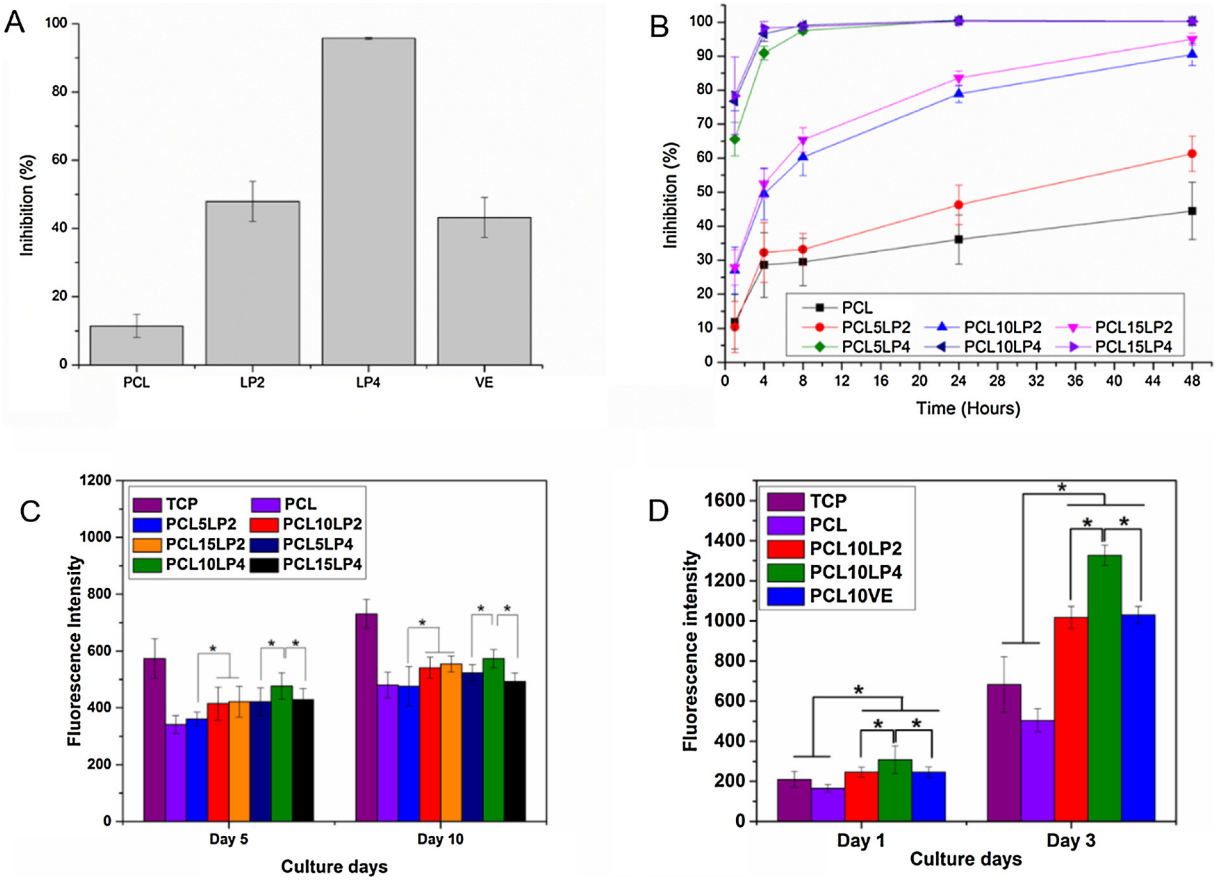

Fig. 5. Free radical inhibition (antioxidant activity) of lignin-PCL copolymers (A) and PCL/lignin-PCL nanofibers (B) by DPPH assay. (C) BMSCs proliferation on different nanofibers and (D) Schwann cells proliferation on different nanofibers after H_2O_2 treatment. (* indicated the significance between two groups, $p < 0.05$, $n = 3$). TCP = tissue culture plate.

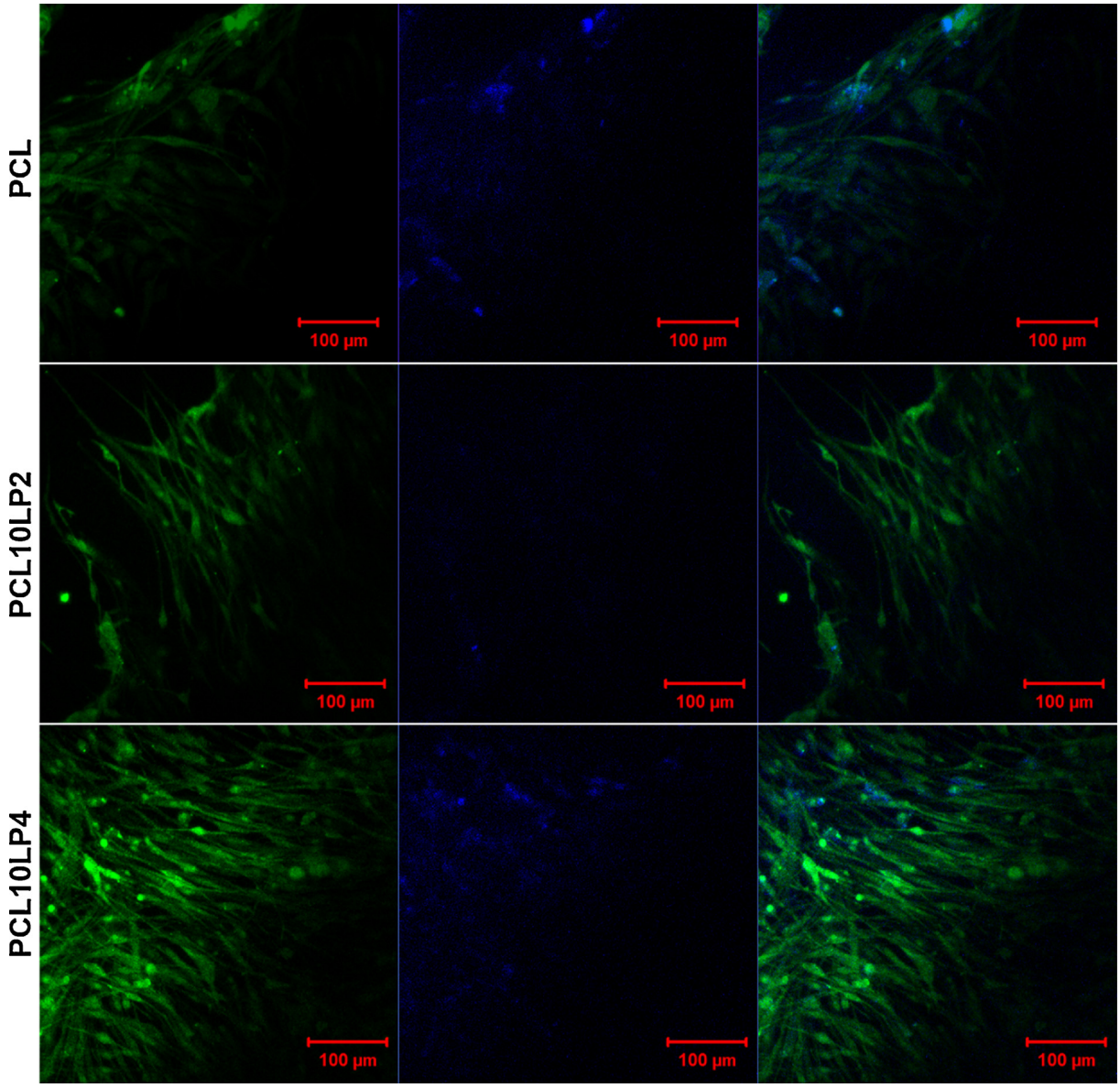

Fig. 6. MBP expression of Schwann cells on different nanofibers. Green color: MBP; Blue color: the nuclei. (For interpretation of the references to colour in this figure legend, the reader is referred to the web version of this article.)

cultured on PCL10LP2 and PCL10LP4 nanofibers were treated with H_2O_2 and their proliferation was evaluated. Exposing cells to H_2O_2 increases intracellular levels of ROS, leading to increased oxidative stress and subsequent cell death due to excessive ROS [36]. As indicated in Fig. 5D, the number of Schwann cells on PCL10LP2, PCL10LP4 and PCL10VE nanofibers surpassed that on pure PCL and TCP in both 1 and 3 days. Furthermore, PCL10LP4 nanofibers resulted in better cell viability than both PCL10LP2 and PCL10VE nanofibers after H_2O_2 treatment. The results suggested that the nanofibers with lignin copolymers exerted protective effect against H_2O_2 toxicity, and LP4 had better antioxidant activity than the commonly-used antioxidant VE, which is consistent with DPPH assay results. This should be attributed to the well-known free radical scavenger, lignin. The hydroxyl and methoxyl functional groups provided hydrogen to terminate oxidation propagation reaction and inhibited cell death caused by excessive ROS resulted of H_2O_2.

3.5. Growth of Schwann cells on PCL/lignin-PCL nanofibers

Schwann cells play a critical role during repair and regeneration of injured peripheral nervous system (PNS) via the synergetic effect with macrophages and neurons [40,43]. Schwann cells that form myelin sheath are capable of up-regulate many myelin gene expressions and secrete diverse neurotrophins to recruit injured neurons and facilitate axon elongation [41,44]. Thus the ability to support growth of Schwann cells is one of the major criteria of scaffolds which determine its successful application for nerve regeneration. Based on the previous results, PCL10LP2 and PCL10LP4 nanofibers were selected for further study. Schwann cells proliferated continuously from day 1 to day 5 on all nanofibers (Fig. S2A). The numbers of cells on PCL10LP2 and PCL10LP4 nanofibers were significantly higher than that on PCL nanofibers on day 1 and day 3, indicating that the addition of LP2 and LP4 favored the proliferation of Schwann cells. The morphology of cells on the nanofibers was evaluated after 7 days incubation by SEM (Fig. S2B). It is observed that the Schwann cells on PCL10LP2 and PCL10LP4 interacted well with the nanofibers and exhibited typical spindle shape with bio-polar extensions. These cells grew in higher density and arranged in bundles. As we know, Schwann cells proliferate and form columns of cells, identified as bands of Büngner to guide the regeneration of axons.

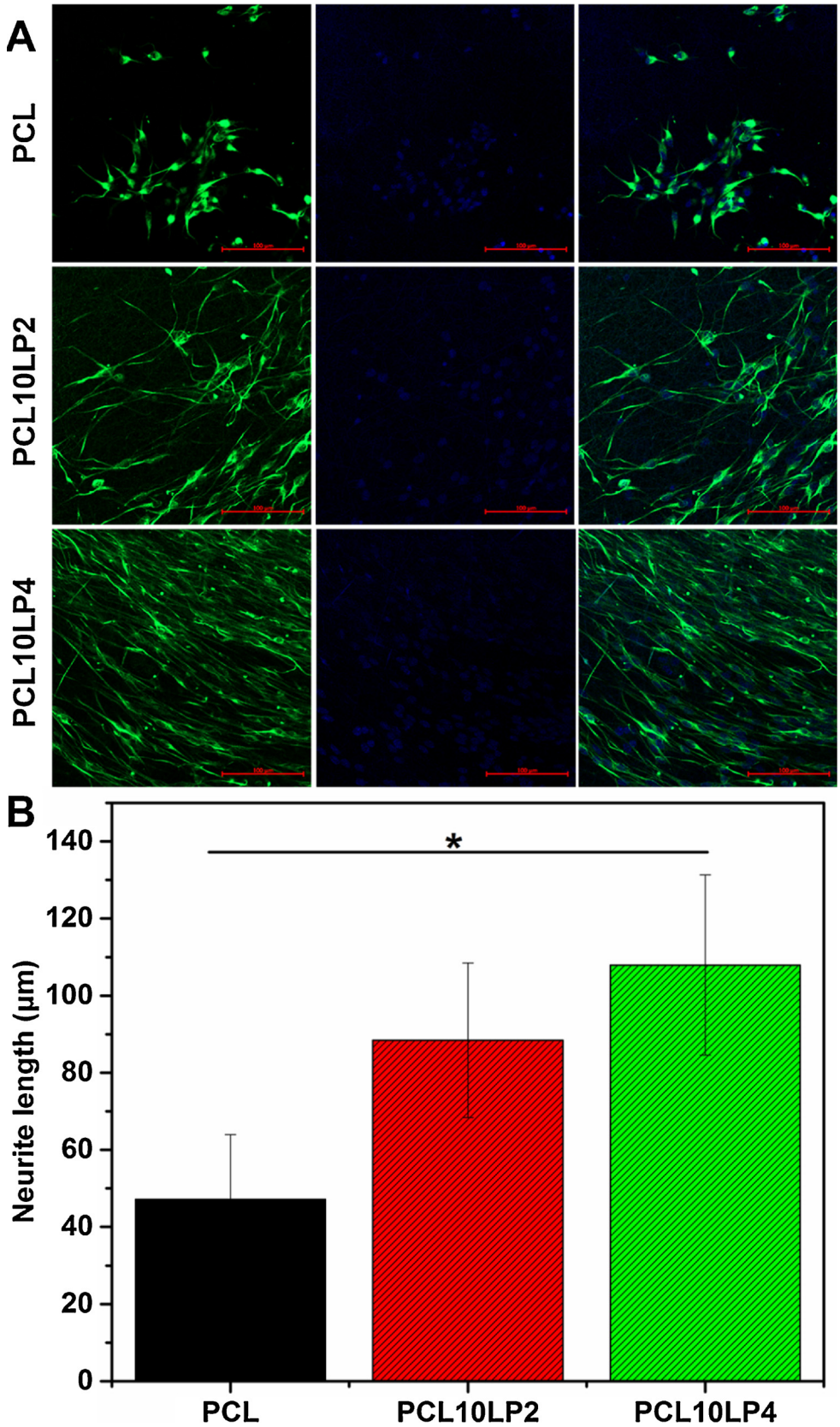

Fig. 7. (A) Fluorescence images of DRG neurons on different nanofibers. Green color: NF160; blue color: nuclei. Scale bar = 100 μm. (B) Neurite length of DRG neurons on different nanofibers after 7 days of culture. (n = 50; * indicated the significance between two different groups, $p < 0.05$.). (For interpretation of the references to colour in this figure legend, the reader is referred to the web version of this article.)

MBP has been shown to be very important during the myelination process and is indispensable for proper formation of myelin thickness and compactness in PNS [45]. As shown in Fig. 6. Schwann cells were able to express MBP on the nanofibrous scaffolds. The cells on PCL10LP4 nanofibers grew in high density with more MBP expression than those on pure PCL and PCL10LP2 nanofibers. Moreover, the cells grew into bundles with a matured morphology on nanofibers with LP2 and LP4. Thus the scaffolds with LP4 copolymers could enhance the expression of MBP, which was beneficial to the formation of myelin sheath. However the possible mechanism has not yet been fully understood, and the complete underlying relationship between lignin and myelination is worth further studying in our next study.

3.6. Growth of primary neurons on PCL/lignin-PCL nanofibers

Neurofilaments are the major group of intermediate filaments which are found mainly in cells of neuronal origin. The expression of the neuronal protein (NF160) by DRG neurons was evaluated to assess its neurite outgrowth on different nanofibers. As shown in Fig. 7A, more neurons were grown on PCL10LP2 and PCL10LP4 nanofibers than pure PCL nanofibers, particularly PCL10LP4. The neurons showed spindle-shaped with long neurites on PCL10LP2 and PCL10LP4 nanofibers, while those on pure PCL nanofibers exhibited round appearance with very short neurites. The neurite length of DRG neurons on different nanofibrous scaffolds are shown in Fig. 7B. The average neurite length of DRG neurons on pure PCL nanofibers was only 46.75 ± 15.63 μm and their longest neurite was up to 67.32 μm. While the mean length of DRG neurons on PCL10LP2 scaffold was 89.21 ± 18.75 μm and the maximum length of neurite observed was up to 135.76 μm. The mean length of neurite projecting on PCL10LP4 nanofibers was the maximum (108.83 ± 21.45 μm) among all samples, with a notably enhanced maximum neurite length of 165.35 μm compared to those on both PCL and PCL10LP2 scaffolds. PCL10LP4 promoted both proliferation and neurite outgrowth of DRG neurons. We believe that the addition of LP4 improved the biocompatibility and antioxidant properties of the nanofibers, which promoted neurons adhesion, proliferation and growth. Consequently, our nanofibrous scaffolds could be a potential substrate for nerve regeneration and functional recovery in peripheral neural tissue engineering.

4. Conclusion

This work opens a new approach for lignin valorization as biomaterials. Here, lignin-PCL copolymers were synthesized by solvent-free ring-opening polymerization, and electrospinning of lignin-PCL copolymers and PCL produced uniformed nanofibers with reinforced mechanical properties. The PCL/lignin-PCL nanofibers exhibited strong free radical scavenging properties and showed capability of protecting cells from oxidative stress effects. Moreover, PCL/lignin-PCL nanofibers were found to promote myelin protein expressions of Schwann cells and stimulate neurite outgrowth of DRG neurons. With suitable mechanical properties, strong antioxidant properties and good biocompatibility, such lignin-PCL copolymers containing nanofibers show their great potential for nerve regeneration and possibly other tissues, especially where cellular oxidative stress is a concern.

Acknowledgements

This research was supported by the National Major Research Program of China (2016YFA0201702 of 2016YFA0201700), National Natural Science Foundation of China (31470941), Science and Technology Commission of Shanghai Municipality (15JC1490100, 15441905100). The authors also gratefully acknowledge the financial support from the Institute of Materials Research and Engineering (IMRE) under the Agency of Science, Technology and Research (A*STAR).

Appendix A. Supplementary data

Supplementary data associated with this article can be found, in the online version, at https://doi.org/10.1016/j.colsurfb.2018.05.021.

References

[1] C. Figueroa-Romero, M. Sadidi, E.L. Feldman, Mechanisms of disease: the oxidative stress theory of diabetic neuropathy, Rev. Endocr. Metab. Disord. 9 (2008) 301–314.
[2] C. Sims-Robinson, J. Hur, J.M. Hayes, J.R. Dauch, P.J. Keller, S.V. Brooks, E.L. Feldman, The role of oxidative stress in nervous system aging, PLoS One 8 (2013) e68011.
[3] A. Areti, V.G. Yerra, V.G.M. Naidu, A. Kumar, Oxidative stress and nerve damage: role in chemotherapy induced peripheral neuropathy, Redox Biol. 2 (2014) 289–295.
[4] J. Friedman, Why is the nervous system vulnerable to oxidative stress? in: N. Gadoth, H.H. Göbel (Eds.), Oxidative Stress and Free Radical Damage in Neurology, Humana Press, Totowa, NJ, 2011, pp. 19–27.
[5] V. Carriel, M. Alaminos, I. Garzón, A. Campos, M. Cornelissen, Tissue engineering of the peripheral nervous system, Expert Rev. Neurother. 14 (2014) 301.
[6] Y. Wu, L. Wang, T. Hu, P.X. Ma, B. Guo, Conductive micropatterned polyurethane films as tissue engineering scaffolds for Schwann cells and PC12 cells, J. Colloid Interface Sci. 518 (2018) 252.
[7] Y. Wu, L. Wang, B. Guo, Y. Shao, P.X. Ma, Electroactive biodegradable polyurethane significantly enhanced Schwann cells myelin gene expression and neurotrophin secretion for peripheral nerve tissue engineering, Biomaterials 87 (2016) 18–31.
[8] M. Turgut, S. Kaplan, Effects of melatonin on peripheral nerve regeneration, Recent Patents Endocr. Metab. Immune Drug Discov. 5 (2011) 100–108.
[9] R.C. Stavisky, J.M. Britt, A. Zuzek, E. Truong, G.D. Bittner, Melatonin enhances the in vitro and in vivo repair of severed rat sciatic axons, Neurosci. Lett. 376 (2005) 98–101.
[10] A.M. Hart, M. Wiberg, G. Terenghi, Pharmacological enhancement of peripheral nerve regeneration in the rat by systemic acetyl-L-carnitine treatment, Neurosci. Lett. 334 (2002) 181–185.
[11] M.R. Farahpour, S.J. Ghayour, Effect of in situ delivery of acetyl-L-carnitine on peripheral nerve regeneration and functional recovery in transected sciatic nerve in rat, Int. J. Surg. 12 (2014) 1409–1415.
[12] M.B. Salles, S.A. Gehrke, S. Koo, S. Allegrini Jr., S.O. Rogero, T.I. Ikeda, A.S. Cruz, E.H. Shinohara, M. Yoshimoto, An alternative to nerve repair using an antioxidant compound: a histological study in rats, J. Mater. Sci.: Mater. Med. 26 (2015) 1–8.
[13] O. Firuzi, R. Miri, M. Tavakkoli, L. Saso, Antioxidant therapy: current status and future prospects, Curr. Med. Chem. 18 (2011) 3871–3888.
[14] X. Zhao, H. Wu, B. Guo, R. Dong, Y. Qiu, P.X. Ma, Antibacterial anti-oxidant electroactive injectable hydrogel as self-healing wound dressing with hemostasis and adhesiveness for cutaneous wound healing, Biomaterials 122 (2017) 34–47.
[15] V. Ugartondo, M. Mitjans, M.P. Vinardell, Applicability of lignins from different sources as antioxidants based on the protective effects on lipid peroxidation induced by oxygen radicals, Ind. Crops Prod. 30 (2009) 184–187.
[16] T. Dizhbite, G. Telysheva, V. Jurkjane, U. Viesturs, Characterization of the radical scavenging activity of lignins—natural antioxidants, Bioresour. Technol. 95 (2004) 309–317.
[17] V. Ugartondo, M. Mitjans, M.P. Vinardell, Comparative antioxidant and cytotoxic effects of lignins from different sources, Bioresour. Technol. 99 (2008) 6683–6687.
[18] Y.Y. Ge, Q. Wei, Z.L. Li, Preparation and evaluation of the free radical scavenging activities of nanoscale lignin biomaterials, Bioresources 9 (2014) 6699–6706.
[19] X.H. Liu, H. Yin, Z.X. Zhang, B.S. Diao, J. Li, Functionalization of lignin through ATRP grafting of poly(2-dimethylaminoethyl methacrylate) for gene delivery, Colloid Surf. B-Biointerfaces 125 (2015) 230–237.
[20] A. Jankovic, S. Erakovic, C. Ristoscu, N. Mihailescu, L. Duta, A. Visan, G.E. Stan, A.C. Popa, M.A. Husanu, C.R. Luculescu, V.V. Srdic, D. Janackovic, V. Miskovic-Stankovic, C. Bleotu, M.C. Chifiriuc, I.N. Mihailescu, Structural and biological evaluation of lignin addition to simple and silver-doped hydroxyapatite thin films synthesized by matrix-assisted pulsed laser evaporation, J. Mater. Sci.-Mater. Med. 26 (2015) 14.
[21] D. Kai, S. Jiang, Z.W. Low, X.J. Loh, Engineering highly stretchable lignin-based electrospun nanofibers for potential biomedical applications, J. Mater. Chem. B 3 (2015) 6194–6204.
[22] S. Jiang, D. Kai, Q.Q. Dou, X.J. Loh, Multi-arm carriers composed of an antioxidant lignin core and poly(glycidyl methacrylate-co-poly(ethylene glycol)methacrylate) derivative arms for highly efficient gene delivery, J. Mater. Chem. B 3 (2015) 6897–6904.
[23] D. Kai, W. Ren, L. Tian, P.L. Chee, Y. Liu, S. Ramakrishna, X.J. Loh, Engineering poly(lactide)–lignin nanofibers with antioxidant activity for biomedical application, ACS Sustain. Chem. Eng. 4 (10) (2016).
[24] D. Kai, Z.W. Low, S.S. Liow, A. Abdul Karim, H. Ye, G. Jin, K. Li, X.J. Loh, Development of lignin supramolecular hydrogels with mechanically responsive and self-healing properties, ACS Sustain. Chem. Eng. 3 (2015) 2160–2169.
[25] L. Tian, M.P. Prabhakaran, J. Hu, M. Chen, F. Besenbacher, S. Ramakrishna, Coaxial electrospun poly (lactic acid)/silk fibroin nanofibers incorporated with nerve growth factor support the differentiation of neuronal stem cells, RSC Adv. 5 (2015) 49838–49848.
[26] L. Tian, M.P. Prabhakaran, J. Hu, M. Chen, F. Besenbacher, S. Ramakrishna, Synergistic effect of topography, surface chemistry and conductivity of the

electrospun nanofibrous scaffold on cellular response of PC12 cells, Colloids Surf. B: Biointerfaces 145 (2016) 420–429.
[27] H. Cao, T. Liu, S.Y. Chew, The application of nanofibrous scaffolds in neural tissue engineering, Adv. Drug Deliv. Rev. 61 (2009) 1055–1064.
[28] L. Ghasemi-Mobarakeh, M.P. Prabhakaran, M. Morshed, M.-H. Nasr-Esfahani, S. Ramakrishna, Electrospun poly (ε-caprolactone)/gelatin nanofibrous scaffolds for nerve tissue engineering, Biomaterials 29 (2008) 4532–4539.
[29] A. Karbalaeimahdi, M. Shahrousvand, H.R. Javadi, M. Ghollasi, F. Norouz, M. Kamali, A. Salimi, Neural differentiation of human induced pluripotent stem cells on polycaprolactone/gelatin bi-electrospun nanofibers, Mater. Sci. Eng. C (2017) 1195–1202.
[30] J. Hu, L. Tian, M.P. Prabhakaran, X. Ding, S. Ramakrishna, Fabrication of nerve growth factor encapsulated aligned poly (ε-caprolactone) nanofibers and their assessment as a potential neural tissue engineering scaffold, Polymers 8 (2016) 54.
[31] R. Augustine, S.K. Nethi, N. Kalarikkal, S. Thomas, C.R. Patra, Electrospun polycaprolactone (PCL) scaffolds embedded with europium hydroxide nanorods (EHNs) with enhanced vascularization and cell proliferation for tissue engineering applications, J. Mater. Chem. B 5 (2017).
[32] S.L. Levengood, A.E. Erickson, F.C. Chang, M. Zhang, Chitosan-poly(caprolactone) nanofibers for skin repair, J. Mater. Chem. B Mater. Biol. Med. 5 (2017) 1822.
[33] E. Bolaina-Lorenzo, C. Martínez-Ramos, M. Monleón-Pradas, W. Herrera-Kao, J.V. Cauich-Rodríguez, J.M. Cervantes-Uc, Electrospun polycaprolactone/chitosan scaffolds for nerve tissue engineering: physicochemical characterization and Schwann cell biocompatibility, Biomed. Mater. 12 (2016) 015008.
[34] N.K. Mohtaram, J. Ko, A. Agbay, D. Rattray, P. O'Neill, A. Rajwani, R. Vansandani, H.L. Thu, B.G. Jun, S. Willerth, Development of a glial cell-derived neurotrophic factor-releasing artificial dura for neural tissue engineering applications, J. Mater. Chem. B 3 (2015) 7974–7985.
[35] D. Kai, K. Zhang, L. Jiang, Z.W. Hua, Z. Li, Z. Zhang, J.L. Xian, Sustainable and antioxidant lignin-polyester copolymers and nanofibers for potential healthcare applications, Acs Sustain. Chem. Eng. 5 (7) (2017).
[36] R. van Lith, E.K. Gregory, J. Yang, M.R. Kibbe, G.A. Ameer, Engineering biodegradable polyester elastomers with antioxidant properties to attenuate oxidative stress in tissues, Biomaterials 35 (2014) 8113–8122.
[37] N. Baheiraei, H. Yeganeh, J. Ai, R. Gharibi, M. Azami, F. Faghihi, Synthesis, characterization and antioxidant activity of a novel electroactive and biodegradable polyurethane for cardiac tissue engineering application, Mater. Sci. Eng. C-Mater. Biol. Appl. 44 (2014) 24–37.
[38] M.P. Prabhakaran, J.S. Venugopal, Mesenchymal stem cell differentiation to neuronal cells on electrospun nanofibrous substrates for nerve tissue engineering, Biomaterials 30 (2009) 4996–5003.
[39] K. Quintiliano, T. Crestani, D. Silveira, V.E. Helfer, A. Rosa, E. Balbueno, D. Steffens, G.P. Jotz, D.A. Pilger, P. Pranke, Neural differentiation of mesenchymal stem cells on scaffolds for nerve tissue engineering applications, Cell. Reprogramming 18 (2016) 369–381.
[40] K. Bhatheja, J. Field, Schwann cells: origins and role in axonal maintenance and regeneration, Int. J. Biochem. Cell Biol. 38 (2006) 1995–1999.
[41] S.P. Frostick, Q. Yin, G.J. Kemp, Schwann cells, neurotrophic factors, and peripheral nerve regeneration, Microsurgery 18 (1998) 397–405.
[42] C.E. Dumont, W. Born, Stimulation of neurite outgrowth in a human nerve scaffold designed for peripheral nerve reconstruction, J. Biomed. Mater. Res. B Appl. Biomater. 73 (2005) 194–202.
[43] K.R. Jessen, R. Mirsky, The origin and development of glial cells in peripheral nerves, Nat. Rev. Neurosci. 6 (2005) 671–682.
[44] J.R. Chan, J.M. Cosgaya, Y.J. Wu, E.M. Shooter, Neurotrophins are key mediators of the myelination program in the peripheral nervous system, Proc. Natl. Acad. Sci. 98 (2001) 14661–14668.
[45] R. Gupta, L. Truong, D. Bear, D. Chafik, E. Modafferi, C.T. Hung, Shear stress alters the expression of myelin-associated glycoprotein (MAG) and myelin basic protein (MBP) in Schwann cells, J. Orthop. Res. 23 (2005) 1232–1239.